8290 *Biochemistry* **2010,** *49,* 8290–8299
DOI: 10.1021/bi1007673

BIOCHEMISTRY
including biophysical chemistry & molecular biology
Article

DsrJ, an Essential Part of the DsrMKJOP Transmembrane Complex in the Purple Sulfur Bacterium *Allochromatium vinosum*, Is an Unusual Triheme Cytochrome *c*[†]

Fabian Grein,[‡] Sofia S. Venceslau,[§] Lilian Schneider,[‡] Peter Hildebrandt,[‖] Smilja Todorovic,[§] Inês A. C. Pereira,[§] and Christiane Dahl*[,‡]

[‡]*Institut für Mikrobiologie & Biotechnologie, Rheinische Friedrich-Wilhelms-Universität Bonn, Meckenheimer Allee 168, D-53115 Bonn, Germany,* [§]*Instituto de Tecnologia Química e Biológica, Universidade Nova de Lisboa, Avenida da Republica, EAN, Apt 127, 2780-157 Oeiras, Portugal, and* [‖]*Technische Universität Berlin, Institut für Chemie, Sekr. PC14, Strasse des 17. Juni 135, 10623 Berlin, Germany*

Received May 14, 2010; Revised Manuscript Received August 19, 2010

ABSTRACT: The DsrMKJOP transmembrane complex has a most important function in dissimilatory sulfur metabolism, not only in many sulfur-oxidizing organisms but also in sulfate-reducing prokaryotes. Here, we focused on an individual component of this complex, the triheme cytochrome *c* DsrJ from the purple sulfur bacterium *Allochromatium vinosum*. In *A. vinosum*, the signal peptide of DsrJ is not cleaved off but serves as a membrane anchor. Sequence analysis suggested the presence of three heme *c* species with bis-His, His/Met, and possibly a very unusual His/Cys ligation. *A. vinosum* DsrJ produced as a recombinant protein in *Escherichia coli* indeed contained three hemes, and electron paramagnetic resonance (EPR) spectroscopy provided evidence of possible, but only partial, His/Cys heme ligation in one of the hemes. This heme shows heterogeneous coordination, with Met being another candidate ligand. Cysteine 46 was replaced with serine using site-directed mutagenesis, with the mutant protein showing a small decrease in the magnitude of the EPR signal attributed to His/Cys coordination, but identical UV−vis and RR spectra. The redox potentials of the hemes in the wild-type protein were determined to be −20, −200, and −220 mV and were found to be virtually identical in the mutant protein. However, in vivo the same ligand exchange led to a dramatically altered phenotype, highlighting the importance of Cys46. Our results suggest that Cys46 may be involved in catalytic sulfur chemistry rather than electron transfer. Additional in vivo experiments showed that DsrJ can be functionally replaced in *A. vinosum* by the homologous protein from the sulfate reducer *Desulfovibrio vulgaris*.

In the purple sulfur bacterium *Allochromatium vinosum*, the degradation of sulfur globules, formed as obligate intermediates during the oxidation of sulfide or thiosulfate, is strictly dependent on the proteins encoded in the *dsr* operon (*1*). *dsr* genes are found not only in sulfur-oxidizing bacteria but also in sulfate- and sulfite-reducing bacteria and archaea. In the latter, dissimilatory sulfite reductase, encoded by the genes *dsrA* and *dsrB*, catalyzes the reduction of sulfite to sulfide as the final step of sulfate reduction. It is believed that the enzyme works in the reverse direction in sulfur-oxidizing bacteria (*2*). While the composition of some of the Dsr proteins differs between sulfate-reducing organisms and sulfur oxidizers (*3*), all prokaryotic genomes that contain genes encoding DsrAB inevitably contain genes encoding the DsrMKJOP transmembrane complex, and it is proposed that these two components interact with each other (*1*, *4*, *5*). Although genes encoding several different transmembrane protein complexes are known in genomes of sulfate-reducing organisms, genes encoding the DsrMKJOP complex are apparently strictly conserved, indicating a vital role in sulfate reduction (*6*).

For the sulfur oxidizer *A. vinosum*, we have previously shown that the degradation of sulfur globules is strictly dependent on the presence of the DsrMKJOP proteins (*3*). The DsrMKJOP protein complex consists of cytoplasmic, membrane integral, and periplasmic components and is predicted to be involved in electron transfer across the membrane (*1*, *7*). DsrM is proposed to be an integral membrane protein with five transmembrane helices and two heme *b* species bound. DsrK is proposed to be a cytoplasmic iron−sulfur protein that is related to the catalytic subunit of heterodisulfide reductase from methanogenic archaea. DsrP is another integral membrane protein with 10 predicted transmembrane helices. Proteins on the periplasmic side of the membrane are DsrO and DsrJ. DsrO is a ferredoxin-like protein and contains a typical signal peptide for translocation across the membrane via the Tat pathway. DsrJ contains an N-terminal signal sequence for the translocation via the Sec pathway, which is not cleaved off in the protein from the archaeal sulfate reducer *Archaeoglobus fulgidus* (*8*). The protein shows no significant homology to other proteins in the database.

The amino acid sequence deduced from the *dsrJ* gene contains three possible Cys-X-X-Cys-His heme binding motifs. In addition, as already pointed out by Pires et al. (*5*) for DsrJ from a dissimilatory sulfate reducer, sequence analysis suggests that the

[†]This work was supported by grants DA 351/3-4 and DA 351/3-5 from the Deutsche Forschungsgemeinschaft, by PTDC/QUI/68368/2006 funded by Fundação para a Ciência e Tecnologia (FCT, MCES, Portugal) and the FEDER program, and by a Luso-German Joint Action funded by the German Academic Exchange Service (DAAD) and Conselho de Reitores das Universidades Portuguesas. S.S.V. is supported by FCT-POCTI Ph.D. Fellowship SFRH/BD/30648/2006.
*To whom correspondence should be addressed: Institut für Mikrobiologie & Biotechnologie, Rheinische Friedrich-Wilhelms-Universität Bonn, Meckenheimer Allee 168, D-53115 Bonn, Germany. Phone: +49 228 732119. Fax: +49 228 737576. E-mail: ChDahl@uni-bonn.de.

FIGURE 1: Sequence alignment of DsrJ proteins, with amino acids 1−132 (*A. vinosum* numbering) shown only. Heme binding motifs are boxed. Putative distal heme ligands are denoted with arrows. Strictly conserved residues are marked with asterisks. Species: *A. vinosum* (Avin), *Magnetococcus* sp. MC-1 (McMC-1), *Thiobacillus denitrificans* (Tden), *Chlorobaculum tepidum* (Ctep), *Desulfovibrio vulgaris* Hildenborough (Dvul), *Desulfovibrio desulfuricans* ATCC 27774 (Ddes), *Archaeoglobus fulgidus* (Aful), *Desulfomicrobium baculatum* (Dmbac), and *Candidatus* Ruthia magnifica (CandRmag).

distal residues responsible for the axial coordination of the hemes may be histidine, methionine, and cysteine (Figure 1). Therefore, DsrJ might be a member of the very small group of unusual multiheme cytochrome *c* forms that have His/Cys-ligated hemes (*5*). The axial ligands of the hemes in *Candidatus* Ruthia magnifica DsrJ may be different since neither the methionines nor the cysteine is conserved (see Discussion).

His/Cys coordination in *c*-type cytochromes was first discovered in the *Rhodovulum sulfidophilum* SoxXA complex involved in thiosulfate oxidation (*9*) and has since also been studied in SoxXA from other organisms (*10*−*12*). Besides this, His/Cys ligation was only proven to be present in one further *c*-type cytochrome. This is PufC, a protein that is associated with the photosynthetic reaction center in *Rh. sulfidophilum* (*13*). Furthermore, the green heme protein from *Halochromatium salexigens* may also contain a His/Cys-ligated heme (*14*). EPR[1] analysis of the purified DsrMKJOP complex from *Desulfovibrio desulfuricans* ATCC 27774 indeed revealed the presence of a His/Cys-ligated heme (*5*), though experimental identification of the ligating cysteine was not conducted. DsrMKJOP has also been purified from *Ar. fulgidus*; however, DsrJ was only present in substochiometric amounts (*8*). This was also the case for preparations from *A. vinosum* that were enriched with DsrK (*1*). In both cases, further specific characterization of DsrJ was not possible. We therefore undertook the production of recombinant *A. vinosum* DsrJ in *Escherichia coli* to obtain sufficient amounts of the protein for its further thorough characterization, in the absence of the other cofactors bound to the DsrMKJOP complex. The unique properties of DsrJ as a cytochrome, namely, the conspicuous His/Cys heme ligation, raise the question of whether its function could involve sulfur redox chemistry, as in SoxXA, rather than just electron transfer with a periplasmic partner. To elucidate this, it is essential to investigate the role of this unusual heme ligation in the physiological function of DsrJ. In this work, we combined site-directed mutagenesis with biophysical measurements to characterize the unusual triheme cytochrome DsrJ. In addition, the importance of the His/Cys heme ligation in DsrJ was investigated in vivo.

[1]Abbreviations: EPR, electronic magnetic resonance; DDM, *n*-dodecyl β-D-maltoside; HS, high-spin; LS, low-spin; Ni-NTA, nickel-nitriloacetic acid; RR, resonance Raman; IPTG, isopropyl β-D-thiogalactopyranoside.

MATERIALS AND METHODS

Bacterial Strains, Media, and Growth Conditions. The bacterial strains and plasmids used are listed in Table S1 of the Supporting Information. *E. coli* strains were cultivated in LB medium (*15*) for molecular cloning or in NZCYM medium (*16*) for production of recombinant protein. *E. coli* DH5α was used for molecular cloning. *A. vinosum* was grown as described previously (*17*). Antibiotics were used at the following concentrations: 100 μg/mL ampicillin, 50 μg/mL kanamycin, and 25 μg/mL chloramphenicol for *E. coli* and 10 μg/mL kanamycin and 50 μg/mL rifampicin for *A. vinosum*.

Recombinant DNA Techniques. Chromosomal DNA of *A. vinosum* and *D. vulgaris* strains were obtained by the standard method as described in ref *18*. Restriction enzymes, T4 ligase, and Pfu DNA polymerase were obtained from Fermentas (St. Leon-Rot, Germany) and used according to the manufacturer's instructions. Cloning oligonucleotides were obtained from Eurofins MWG (Ebersberg, Germany).

Cloning of the dsrJ Gene and Construction of a dsrJC46S Mutant. The gene *dsrJ* was amplified from chromosomal *A. vinosum* DNA either with or without the native signal peptide, and amplified products were cloned in pET22b, resulting in plasmids pETJHisSP and pETJHis.

For expression of the soluble protein with a C-terminal Strep tag, plasmid pPRIBApelBJStrep was constructed. With this construct, production of the proper holoprotein was not achieved. Therefore, the vector was digested with *Nco*I and *Hin*dIII, and the insert was transferred back into the pET22b backbone, resulting in plasmid pETJStrep. This plasmid encoded soluble DsrJ, including a C-terminal Strep tag, and provided a low level of basal expression because of the lacT7 promoter in pET22b in contrast to the T7 promoter in pPRIBApelBStrep. The Cys46Ser point mutation was introduced into *dsrJ* via gene splicing by overlap extension (*19*).

Production and Purification of DsrJ from E. coli. For the production of recombinant DsrJ, *E. coli* BL21(DE3) was first transformed with the pEC86 plasmid that provides the expression of the genes encoded in the *ccm* operon under aerobic conditions (*20*) and then transformed with the appropriate plasmid used for expression of *dsrJ*; 400 mL of medium in a nonbaffled Erlenmeyer flask was inoculated with a single colony of the appropriate clone and grown at 37 °C and 180 rpm agitation for 16−18 h without any induction. The cells were harvested by centrifugation for 15 min at 10000*g*, washed with buffer W [100 mM Tris-HCl and 150 mM NaCl (pH 7.5)], and stored at −20 or −70 °C until further use. For purification, the cells were thawed, resuspended in buffer W, and lysed by sonication. To remove insoluble components, the extract was centrifuged for 30 min at 25000*g* and 4 °C. The supernatant was applied to an affinity chromatography column (Strep-Tactin Superflow, IBA BioTagnology, Göttingen, Germany). The protein was frozen and used for EPR and RR spectroscopy or further purified for heme quantification, redox titration, or UV−vis spectroscopy. This was achieved by immediate application of the protein to a Superdex 75 pg gel filtration column that was equilibrated with 50 mM NaH_2PO_4 (pH 7.0). Monomeric DsrJ eluted between 75 and 78 mL. Fractions were combined, frozen in liquid nitrogen, and stored at −70 °C until they were used.

Protein Techniques. Tricine SDS−PAGE was conducted by the method of Schägger (*21*). Immunoblot analysis was conducted as described previously (*1*). Heme staining in acrylamide gels was conducted by the method of Thomas et al. (*22*). The heme concentration was determined by the method of Berry and Trumpower (*23*). The protein concentration of purified protein was determined with the BCA kit from Pierce (Rockford, IL).

Mass Spectrometry. Data were obtained by the Mass Spectrometry Laboratory, Analytical Services Unit, Instituto de Tecnologia Química e Biológica, Universidade Nova de Lisboa. Protein samples (5 μL) were desalted, concentrated, and eluted using R1 (RP-C4 equivalent) microcolumns. Proteins were eluted directly onto the MALDI plate with sinapinic acid (10 mg/mL) using 50% (v/v) acetonitrile and 5% (v/v) formic acid. Mass spectra were recorded in the positive linear MS mode using a MALDI-TOF/TOF, Applied Biosystems, model 4800 instrument (PO 01MS).

Spectroscopic Methods. UV−vis spectra were recorded in an analytic Jena Specord 210 spectrophotometer. EPR spectra were recorded using a Bruker EMX spectrometer equipped with an ESR 900 continuous-flow helium cryostat from Oxford Instruments. RR measurements were performed with a confocal microscope coupled to a Raman spectrometer (Jobin Yvon U1000). Samples were placed in a quartz rotating cell, excited with a 413 or 647 nm line from a krypton ion laser (Coherent Innova 302), and measured with a 5 mW laser power and accumulation times of 60 s at room temperature. After polynomial background subtraction, the positions and line widths of the Raman bands were determined by component analysis (*24*).

Redox Titrations. Redox titrations were performed inside an anaerobic glovebox. The following redox mediators (final concentration of 1 μM) were added to the protein in 50 mM NaH_2PO_4 (pH 7.0): dichlorophenolindophenol, 1,2-naphthoquinone, duroquinone, indigotrisulfonate, 2-hydroxy-1,4-naphthoquinone, anthraquinone 2-sulfonate, neutral red, benzyl viologen, and methyl viologen.

Table 1: Sulfur Accumulation and Oxidation to Sulfate of *A. vinosum* Wild-Type and Δ*dsrJ* Strains Complemented with Various *dsrJ* Genes

strain	[sulfur] (mM) 4 h	[sulfur] (mM) 24 h	[sulfur] (mM) 48 h	[sulfate] (mM) 4 h	[sulfate] (mM) 24 h	[sulfate] (mM) 48 h
wild type[a]	0.72	0.11	0.03	0.3	0.95	1.01
Δ*dsrJ* and *dsrJ* wild type	0.94	0.19	0.17	0	0.73	0.72
Δ*dsrJ* and *dsrJC46S*	1.1	0.96	0.87	0	0.16	0.19
Δ*dsrJ* and *dsrJ D. vulgaris*	0.77	0.11	0.06	0	0.71	0.78

[a]The protein contents were 100−130 μg/mL at the start of the experiment. Data for *A. vinosum* wild type are from the experiment described in ref *25*.

The protein was reduced stepwise by the use of buffered sodium dithionite as a reductant. The absorption spectra were recorded with a Perkin-Elmer Lambda 11 spectrophotometer. Redox titrations were followed both at the reduced Soret and at the α bands, giving identical results. The changes in absorbance at the Soret band of the hemes (417.5 nm) were corrected for the corresponding isosbestic points (388 and 436 nm). The redox potential was measured with a Mettler Toledo InLab redox micro redox electrode and referenced to the standard hydrogen electrode.

Construction and Characterization of Complemented A. vinosum Δ*dsrJ Mutants*. Complementation of an *A. vinosum* Δ*dsrJ* mutant (*3*) was conducted with *A. vinosum dsrJ*, *dsrJC46S*, and *dsrJ* carrying a C-terminal His tag coding sequence. Furthermore, the complementation was conducted with *dsrJ* from *D. vulgaris*. The constructs including the native signal peptide were cloned downstream of the *dsr* promoter region in pBBR1MCS2-L (*25*) where they replaced the *dsrL* gene. Complementation plasmids were transferred from *E. coli* S17-1 to *A. vinosum* Δ*dsrJ* by conjugation (*26*). Transconjugants were selected on plates with modified RCV medium (*27*) supplemented with kanamycin as described in ref *28*.

Photolithoautotrophic growth of the mutant strains was examined in batch culture under continuous illumination at 30 °C essentially as described by Prange et al. (*29*) in a medium containing carbonate and sulfide as the sole sulfur compound; 250 mL of a photoheterotrophically grown stationary-phase culture was harvested (5900*g* for 10 min), and the cell material was used to inoculate 1 L of modified Pfennig's medium in a fermenter. The experiments were started by the addition of approximately 2 mM sulfide from a sterile stock solution (1 M). Sulfur compounds were assessed by HPLC (Thermo Separation Products TSP) using the methods of Rethmeier et al. (*30*). Elemental sulfur was assessed by cyanolysis (*31*).

Production and Purification of DsrJ from A. vinosum. For the purification of DsrJ from *A. vinosum*, Δ*dsrJ*+Jhis cells (Table 1) were grown in RCV medium in 1 L flasks. Five-day-old cultures were induced with 2 mM sulfide and harvested after 3 h. Cells were harvested by centrifugation, washed with buffer A [50 mM NaH_2PO_4 and 300 mM NaCl (pH 7.5)], frozen, and stored at −20 or −70 °C until further use. For purification, cells were thawed, resuspended in buffer A, and lysed by sonication. Insoluble components were removed by centrifugation, and the membrane fraction was prepared from the supernatant by ultracentrifugation at 145000*g* for 3 h at 4 °C. Membranes were solubilized at least twice with 2% dodecyl maltoside (DDM) (w/v) with gentle stirring on ice for several hours or overnight followed by another ultracentrifugation. The supernatant was

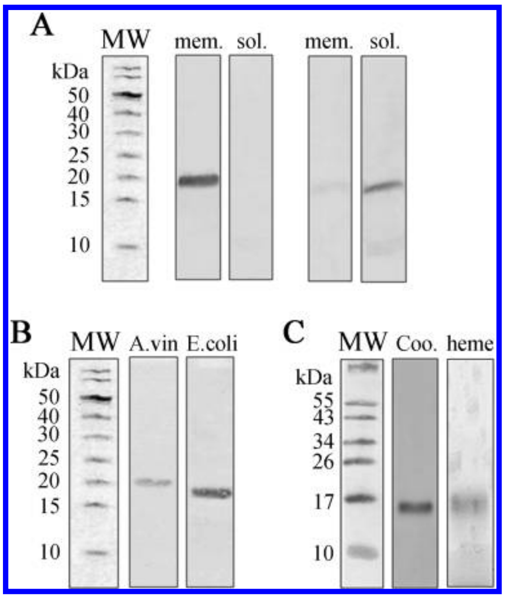

FIGURE 2: Tricine SDS−PAGE and Western blot using an anti-DsrJ antibody. (A) Western blot analysis of fractions of *E. coli* producing DsrJ with the native signal peptide (left) and with the PelB leader (right). mem denotes the membrane fraction, and sol denotes the soluble fraction. (B) Western blot analysis: A.vin, *A. vinosum* fraction enriched with Dsr; *E. coli*, purified recombinant DsrJ without the signal peptide from *E. coli*. (C) SDS−PAGE analysis of purified recombinant DsrJ: Coo, Coomassie stain; heme, heme stain; MW, molecular mass markers.

supplemented with 15 mM imidazole and applied to a Ni-NTA agarose column (Qiagen, Hilden). The column was washed with a stepwise gradient from 20 to 80 mM imidazole in buffer A supplied with 0.1% DDM, and the protein was eluted with 250 mM imidazole in buffer A. The eluted protein was concentrated and desalted by the use of a HiTrap desalting column.

RESULTS

Production and Purification of DsrJ from E. coli and A. vinosum. First trials for heterologous production of DsrJ in *E. coli* have been described, but satisfying production of holoprotein was not achieved (*1*). We therefore started with improving the production of DsrJ and compared the yields, cellular localization, and purity of recombinant DsrJ when joined with its native signal peptide or when produced as a fusion protein with the PelB leader, the signal peptide of the pectate lyase from *Erwinia carotovora*. The proteins were combined with a carboxy-terminal hexahistidine or Strep tag to facilitate purification and detection. Successful production of holoprotein was achieved by coexpression of the *ccm* genes from pEC86 (*20*).

When DsrJ was produced in *E. coli* with its native signal peptide, the protein was not processed and exclusively found in the membrane fraction. The molecular mass as judged by sodium dodecyl sulfate−polyacrylamide gel electrophoresis (SDS−PAGE) (Figure 2A) was in accordance with the nonprocessed form of the protein. When the PelB leader was used instead of the native signal peptide, the protein was processed and present in the soluble cell fraction (Figure 2A). His-tagged DsrJ with its native signal peptide was also produced in *A. vinosum* and enriched via nickel-chelate affinity chromatography. Under these conditions, DsrJ was identified as a 19 kDa protein by SDS−PAGE via an anti-DsrJ antiserum (Figure 2B). This molecular mass was in perfect accordance with that predicted for the His-tagged *c*-type cytochrome, including its signal peptide, while the calculated molecular mass of the processed form would have been only 16.6 kDa. The apparent molecular mass of native DsrJ, as judged by SDS−PAGE and comparison with the soluble version from *E. coli* after removal of the PelB leader, allowed us to conclude that the signal peptide of DsrJ is not cleaved off in *A. vinosum*.

For the following experiments, we chose to produce the soluble version of DsrJ to facilitate purification and subsequent characterization. A Strep tag at the C-terminus was used instead of the hexahistidine tag to exclude possible interactions of additional histidines with the natural heme iron ligands. Proper maturation to a fully heme-loaded DsrJ holoprotein was found to be absolutely dependent on slow production of the recombinant protein in *E. coli*. The required minimum expression level was achieved by the use of the lacT7 promoter in the pET22b vector and by completely omitting induction. The thus produced DsrJ was successfully purified to homogeneity by affinity chromatography and gel filtration (Figure 2C); 820 μg of pure DsrJ was obtained from 1 L of expression culture. To investigate the role of the cysteine heme coordination, a mutant form of the protein, DsrJC46S, in which Cys46 was replaced with a serine, was also produced. This amino acid substitution, which only replaces a sulfur atom with oxygen, was chosen to address the specific role of this sulfur atom without changing other stereochemical properties.

Characterization of DsrJ and DsrJC46S. DsrJ was first characterized by UV−vis spectroscopy. The protein as isolated is completely oxidized as addition of hexacyanoferrate did not alter the spectrum (not shown). The spectrum of oxidized DsrJ is typical for LS ferric heme and revealed a Soret peak at 408 nm. Upon reduction, the peak shifted to 417.5 nm and α and β peaks were observed at 551 and 523 nm, respectively. An additional weak signal at 650 nm was detected in the oxidized and reduced state (Figure 3A). The nature of this band is not completely clear. However, resonance Raman (RR) spectra obtained with 647 nm excitation reveal only the presence of non-totally symmetric modes, indicating that the 650 nm electronic absorption band belongs to a Q-band (α/β transitions) (see the Supporting Information). Similar bands are frequently present in the spectra of ferric P450 cytochromes in which Cys is a proximal ligand (*32*). Some authors have correlated this band with five-coordinate high-spin (HS) species, but it is also present in some substrate-bound LS P450 cytochromes, and also in some Cys/His P450 mutants (*33*). The presence of HS hemes in DsrJ is ruled out by both EPR and RR spectroscopy (see below the RR data with 413 nm excitation), but the fact that the 650 nm band is also present in the C46S mutant also argues against it being due to Cys coordination. Thus, it is not clear at this point which heme gives origin to this band.

Heme quantification revealed 2.6 mol of heme *c*/mol of DsrJ for the unaltered protein and 2.7 mol of heme *c*/mol of DsrJC46S. Final proof that the holocytochrome was properly and completely loaded with heme was achieved by mass spectrometry. The obtained spectrum showed that the vast majority of protein binds three hemes (as the mass differed by 1838 Da from the protein without heme), while only minor peaks were detected for DsrJ with two (1221 Da), one (607 Da), and zero hemes bound. DsrJC46S was also purified as a three-heme cytochrome as confirmed by mass spectroscopy. The UV−vis spectrum of the purified mutated protein was unaltered as compared to that of original DsrJ, including the presence of the 650 nm band (Figure 3B).

X-Band EPR Spectroscopy. The EPR spectrum of purified DsrJ (Figure 4A-1) revealed signals for LS species at *g* values of

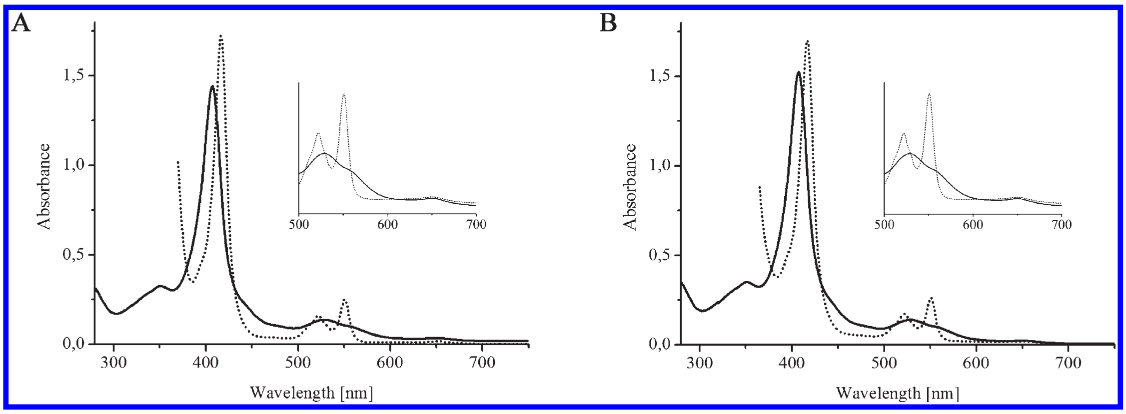

FIGURE 3: UV−vis spectra of purified recombinant DsrJ (A) and DsrJC46S (B) in the oxidized (—) and reduced form (---). The insets are close-up views of the 500−700 nm region.

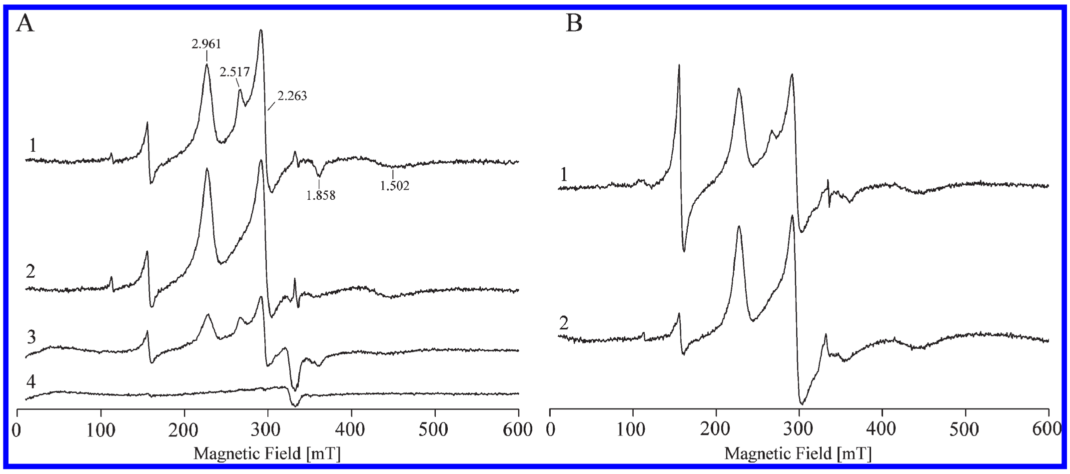

FIGURE 4: EPR spectra of purified recombinant DsrJ. (A) As-isolated samples and (B) redox-cycled samples: (1) wild-type DsrJ (130 μM), (2) DsrJC46S (180 μM), (3) wild-type DsrJ reduced with ascorbate, and (4) wild-type DsrJ reduced with dithionite. Experimental conditions: microwave frequency, 9.38 GHz; microwave power, 2 mW; modulation frequency, 100 kHz; modulation amplitude, 1 mT; temperature, 10 (A) or 15 K (B).

2.961 and 2.517 (g_{max}), 2.263 (g_{med}), and 1.858 and 1.502 (g_{min}). The 2.961, 2.263, and 1.1502 values are in the range typically found for LS hemes with His/His or His/Met ligation (*9*), while the signals at 2.517 and 1.858 are outside of this range. The latter signal was provisionally attributed to a His/Cys-ligated heme because a comparable signal was also detected for the DsrMKJOP complex from *D. desulfuricans* and proposed to be due to a His/Cys-ligated heme in DsrJ (*5*), and similar *g* values have been observed for the His/Cys-ligated hemes in SoxXA and PufC from *Rh. sulfidophilum* (*9*, *13*). However, spectral simulation of the two g_{max} = 2.961 and g_{max} = 2.517 species indicates that the latter one accounts for substantially less than one heme (a maximum of ~0.5−0.6 heme), suggesting that coordination of this heme is heterogeneous.

In the EPR spectrum of DsrJC46S, the magnitudes of the signals at 2.517 and 1.858 that are possibly due to a His/Cys-ligated heme were decreased (Figure 4A-2). Spectral integration of the DsrJ and DsrJC46S EPR signals shows very similar relative intensity, which indicates that the reduced intensity of the g_{max} = 2.517 signal is compensated by an increase in the g_{max} = 2.961 signal. Upon treatment of the wild-type protein with the mild reductant ascorbate, the magnitudes of both the g_{max} = 2.961 signal and the g_{max} = 2.517 signal decreased (Figure 4A-3). However, the relative contribution of the g_{max} = 2.517 signal seems to be larger than in the oxidized sample, suggesting that the heme responsible for this signal may have a lower potential than the others. Nevertheless, the partial reduction of this heme by ascorbate indicates that it is redox active and does not have an extremely low redox potential, as observed for the His/Cys-coordinated heme in SoxXA from *Rh. sulfidophilum* and *Paracoccus pantotrophus* (*9*, *34*) or DsrJ from *D. desulfuricans* (*5*). This conclusion was corroborated upon reduction with the strong reductant dithionite, which leads to complete reduction of the hemes as observed by EPR spectroscopy (Figure 4A-4). Upon reoxidation of the wild-type protein (Figure 4B-1), the intensity of the g_{max} = 2.517 signal decreased, accounting for a maximum of 0.2−0.3 heme in the redox-cycled protein. Upon comparison of spectral simulations of the redox-cycled wild-type and mutant proteins, the difference in the g_{max} = 2.517 signal intensity is on the order of only 0.1 heme. This further indicates that possible coordination of one of the hemes by Cys46 is only partial, and that ligand switching may occur during reduction as observed for cd_1 nitrite reductase (*35*−*37*). Because HS heme features are not observed by EPR or RR (see below), another residue should also coordinate this heme, and a likely candidate is the second conserved methionine. Notably, a HS heme is also not observed in DsrJC46S by EPR or RR, suggesting that the iron in the corresponding heme is still six-coordinate, although the presence of a small amount of HS heme cannot be ruled out.

RR Spectroscopy. The high-frequency region RR spectra of as-isolated DsrJ obtained upon Soret band excitation reveal

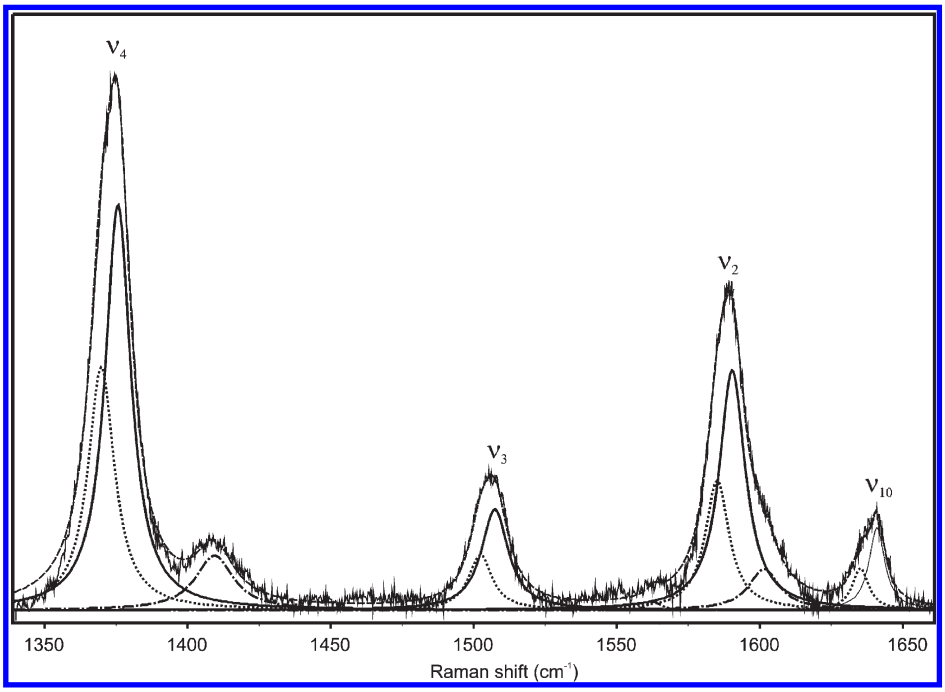

FIGURE 5: High-frequency RR spectra of DsrJ. Experimental spectrum obtained with a 413 nm excitation, a 5 mW laser power, 75 μM ferric protein, and a 60 s accumulation time at room temperature. Component spectra: dotted line for ν_4 at 1370 cm^{-1}, ν_3 at 1502 cm^{-1}, ν_2 at 1584 cm^{-1}, and ν_{10} at 1635 cm^{-1}, solid line for ν_4 at 1375 cm^{-1}, ν_3 at 1507 cm^{-1}, ν_2 at 1590 cm^{-1}, and ν_{10} at 1640 cm^{-1}, and dashed line for the overall component spectrum.

typical fingerprint bands of ferric LS cytochrome *c* (Figure 5). These modes, however, appear broadened and asymmetric. The component analysis revealed two bands for each mode with line widths consistent with the respective natural line widths (*38*), which we attribute to two heme populations with different coordination patterns. The population with upshifted marker band frequencies (ν_4 at 1375 cm^{-1}, ν_3 at 1507 cm^{-1}, ν_2 at 1590 cm^{-1}, and ν_{10} at 1640 cm^{-1}) bears strong spectroscopic similarities to imidazole complexes of horse heart cytochrome *c* or ferric cytochrome *c*″ (*38*) and can therefore be assigned to the bis-His hemes. The RR fingerprint of the second population (ν_4 at 1370 cm^{-1}, ν_3 at 1502 cm^{-1}, ν_2 at 1584 cm^{-1}, and ν_{10} at 1635 cm^{-1}), also encountered in various cytochrome *c* species carrying the His/Met axial ligation, such as mitochondrial cytochrome *c*, FixL (*Bradyrhizobium japonicum*), or cytochrome *c* from subunit II of *caa*$_3$ oxygen reductase (*Rhodothermus marinus*), indicates His/Met coordination (*39*). Because there are no reported RR spectral parameters for the His/Cys coordination pattern in the literature, the spin population to which it may contribute (His/His or His/Met) is not clear. However, on the basis of the analogy with RR spectra of LS ferric cytochrome P450, with proximal Cys and distal H_2O/OH ligation, or substrate-bound cytochrome P450, we expect a high degree of similarity of the possible His/Cys heme population in DsrJ with Met/His-coordinated heme (*24*). Mutation of axial Cys46 to Ser had no consequences with respect to the RR spectra. Component analysis revealed the same band positions, line widths, and relative intensity ratios of the marker bands for the two proteins.

Redox Titrations. A redox titration monitoring the absorbance changes in the Soret band at 417.5 nm by visible spectroscopy was performed to estimate the E_m of the triheme DsrJ. The hemes start to be reduced at approximately 50 mV and are fully reduced at approximately −200 mV. The experimental points show two redox transitions with a relative proportion of 2:1 and can be fitted by adding three Nernst equations with redox potentials of −20, −200, and −220 mV in a 1:1:1 ratio. This simplified interpretation of the results most likely does not reflect the actual redox potential of the three hemes, as several confounding factors are likely present. (i) The differently coordinated hemes may have distinct extinction coefficients and will therefore contribute differently to the absorbance at any given wavelength. (ii) It is likely that there is redox cooperativity between the hemes, as commonly observed in multiheme cytochromes (*40*), which affects the macroscopic redox potentials determined in the redox titration. In particular, there seems to be cooperativity in the two hemes being reduced around −210 mV, suggesting a close contact between them. Because the proposed His and Met axial ligands are adjacent in the sequence (Figure 1), the hemes to which they coordinate will most likely be closer in space and are good candidates for this interacting heme pair. Interestingly, the redox titration of the Cys46Ser mutant protein yielded very similar results, revealing that the mutation did not have any detectable effect on the redox potential of the hemes (Figure 6). This further indicates, as suggested from the EPR results, that only a small fraction of one heme may be coordinated by His/Cys, and this fraction may decrease with reduction. Furthermore, these results suggest that a possible His/Cys-coordinated heme is not likely to be involved in a redox function.

As already pointed out, DsrJ is thought to be associated with DsrMKOP in *A. vinosum* (*1*). Indeed, in a membrane preparation of *A. vinosum* Δ*dsrJ* with pBBRJHis that was enriched with DsrJ by nickel-chelate affinity chromatography, co-purification of DsrM, DsrK, and DsrO was verified using specific antisera against these proteins (not shown). The presence of DsrP could not be shown because an antibody was not available. Because the in vivo situation is well-mirrored in this preparation, we investigated the redox behavior of the heme *c* species in the sample. In close analogy to our redox potentiometric results obtained for recombinant DsrJ alone, the heme *c* species in the DsrMKJOP complex preparation from *A. vinosum* started to be reduced at 20 mV and were fully reduced at −240 mV. Lowering the potential even

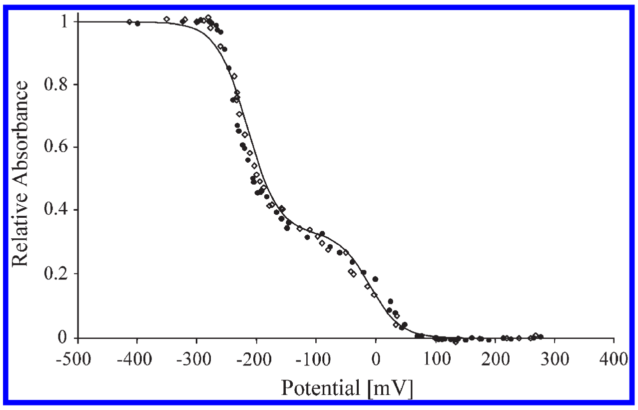

FIGURE 6: Redox titration of wt DsrJ (●) and DsrJC46S (◇) followed by UV−visible spectroscopy at 417.5 nm. The solid line corresponds to a theoretical simulation obtained by adding three Nernst equations with redox potentials of −20, −200, and −220 mV.

further to −500 mV by the use of titanium(III) citrate did not lead to further reduction (not shown).

Role of the DsrJ His/Cys-Ligated Heme in Vivo. To examine the role that DsrJ cysteine 46 plays in vivo, an *A. vinosum* Δ*dsrJ* mutant strain lacking a functional *dsrJ* gene (*3*) was complemented in trans with genes encoding either unaltered DsrJ or DsrJC46S. When grown photolithoautotrophically on 1−2 mM sulfide, *A. vinosum* wild type rapidly forms sulfur globules. Under the standard conditions used in our laboratory (*29*), the stored sulfur is usually oxidized to the end product sulfate within 24 h. In contrast, the Δ*dsrJ* mutant is completely unable to oxidize intracellular sulfur (*3*). The phenotype of the *A. vinosum* Δ*dsrJ* mutant complemented with unaltered *dsrJ* under the control of the *dsr* promoter (*25*) was comparable to the wild type (Table 1). However, when the mutant lacking *dsrJ* was complemented with the gene encoding DsrJ carrying the Cys46-Ser mutation, the ability to further metabolize stored sulfur was dramatically impaired because after 24 h only 0.16 mM sulfate was produced and even after 48 h only 0.19 mM sulfate was produced (Table 1). This is especially remarkable because spectroscopic and redox potentiometric analysis did not reveal striking differences between the wild type and the mutant protein.

Complementation of A. vinosum Δ*dsrJ with dsrJ from D. vulgaris*. To investigate functional similarity between DsrJ from the sulfide oxidizer *A. vinosum* and the sulfate reducer *D. vulgaris*, we tested whether the *A. vinosum* wild-type phenotype can be restored by the complementation of *A. vinosum* Δ*dsrJ* with *dsrJ* from *D. vulgaris*. The complemented strain was able to oxidize sulfide and accumulated sulfur globules rapidly (Table 1). The sulfur globules were degraded within 24 h, and 0.71 mM sulfate was produced, showing the capacity of Δ*dsrJ* and *dsrJ D. vulgaris* to oxidize sulfur, and thus to restore the wild-type phenotype.

DISCUSSION

In this study, we achieved the heterologous production of a single component of the DsrMKJOP transmembrane complex from *A. vinosum* in *E. coli*. DsrJ was successfully produced as a soluble protein, transported into the periplasm, and processed and properly maturated to a triheme cytochrome *c*. Minimal expression without induction with IPTG and the coexpression of the *E. coli ccm* genes from plasmid pEC86 (*20*) were found to be important factors for correct maturation. We have unambiguously shown that the native signal peptide of DsrJ serves as a membrane anchor for the protein when it is produced in *E. coli*. We also propose this situation for DsrJ in *A. vinosum* because the signal peptide is not cleaved off in vivo. A similar retainment of the signal peptide as a membrane anchor has been shown for the analogous protein from *Ar. fulgidus* (*8*).

DsrJ was studied by UV−vis, EPR, and RR spectroscopies, as well as by mass spectrometry and redox potentiometry. We also investigated the existence of an unusual His/Cys heme axial coordination and its possible role by site-directed mutagenesis followed by biochemical and biophysical characterization of the protein. These studies were further complemented by in vivo experiments.

For the identification and characterization of axial heme ligands in cytochromes, point mutations are typically introduced to change the putative native ligands to other well-established heme ligands like histidine or methionine. Depending on the introduced mutation, this usually leads to an alteration of the midpoint redox potentials (*13*, *41*, *42*). Compared to those of histidine/cysteine- or bis-histidine-ligated hemes, the midpoint potentials of His/Met-ligated hemes are typically higher (*43*, *44*). Another strategy is the replacement of the natural ligand with small residues like alanine and glycine that cannot ligate the heme iron (*45*, *46*). In this study, we used a different strategy to identify and examine the potential role of a cysteine as the sixth axial ligand of one of the three hemes in DsrJ. Cysteine 46 was replaced with serine. These two amino acids only differ by the presence of an oxygen atom in serine instead of sulfur in cysteine. The Cys46Ser mutation had no effect on the visible and RR spectra of the protein or on the heme's redox behavior. However, a small effect was detected by EPR spectroscopy where a g_{max} = 2.517 signal that may be attributed to a thiolate-coordinated heme exhibited decreased intensity in the mutant. The intensity of this signal was also decreased in the wild-type protein following reduction and reoxidation. Our results suggest that Cys coordination is only partial, with this heme having heterogeneous coordination, possibly by a second conserved methionine.

Redox titrations revealed the presence of three redox species in DsrJ with midpoint potentials of −20, −200, and −220 mV. Given the apparent heterogeneity in the heme coordination of DsrJ, which may also change upon reduction, we do not attempt to attribute these redox transitions to individual hemes. The His/Cys-ligated heme present in the purified DsrMKJOP complex from *D. desulfuricans* was still not fully reduced at −400 mV (*5*). While the midpoint potential of the His/Cys-coordinated heme in PufC from *Rh. sulfidophilum* was determined to be −160 ± 10 mV (*13*), the potentials of His/Cys-ligated hemes in SoxXA from *Chlorobaculum* (formerly *Chlorobium*) *tepidum*, *P. pantotrophus*, and *Starkeya novella* are all below −400 mV (*11*, *34*, *47*). For *A. vinosum* DsrJ, we can confidently exclude a very negative midpoint potential or redox inactivity of any of the hemes. By EPR analysis, the putatively His/Cys-ligated heme (g_{max} = 2.517) already started to be reduced upon addition of the mild reductant ascorbate and could be fully reduced with dithionite (Figure 4A-3,4). However, care must been taken in extrapolating redox potentiometric analysis of a single component to the in vivo situation within the complex. Therefore, we also analyzed an *A. vinosum* membrane fraction that was enriched in DsrMKJOP and found a redox behavior of the heme *c* species that was very similar to that of the isolated recombinant DsrJ.

The role and significance of His/Cys ligation in *c*-type cytochromes are not yet understood. It has been most studied in SoxXA proteins, which are involved in thiosulfate oxidation (*48*, *49*).

The catalytic subunit SoxA is a diheme protein in *Rh. sulfidophilum* and *P. pantotrophus* (*9*, *12*), while heme 1 is missing in *S. novella* and *C. tepidum* (*10*, *11*). In all cases, heme 2 or the single heme corresponding to heme 2 has His/Cys ligation and is characterized by a very negative midpoint potential (*11*, *34*, *47*). When present, heme 1 is also a His/Cys-ligated heme and is redox inactive (*9*, *34*). In SoxXA from *P. pantotrophus*, heme 1 remains oxidized even at potentials of −800 mV (*34*), and structural investigations of the proteins from *Rh. sulfidophilum* and *P. pantotrophus* revealed that the distance between heme 1 and heme 2 is too long for electron transfer (*50*, *51*). Redox inactivity and the fact that heme 1 is replaced by a disulfide bridge in the protein from *S. novella* (*10*) lead to the conclusion that this His/Cys-ligated heme is not important for the catalytic function of SoxXA (*34*). Heme 2 has an exceptionally low midpoint potential of less than −400 mV in all SoxXA proteins studied so far and is characterized by the modification of cysteine to a persulfide that ligates the heme (*9*, *50*). This heme is the catalytic active site. The substrate thiosulfate is bound to the ligating cysteine, resulting in a SoxA-thiocysteine-*S*-sulfate intermediate. The sulfur−sulfur bond is polarized by an arginine, and the thiosulfate may be bound to SoxYZ (*50*). It is interesting to note that there is a conserved arginine in the vicinity of cysteine 46 in DsrJ (Figure 1).

So far, we have no evidence of a persulfide modification of the cysteine in DsrJ. We observed that possible His/Cys coordination for one of the hemes seems to be only partial, and that the Cys46Ser mutation has almost no effect on the redox behavior of the protein in vitro. However, in vivo this ligand exchange led to a protein that was functionally strongly impaired. Thus, it appears rather unlikely that the dramatic effect of ligand exchange in vivo would be due solely to interrupted electron transport. Our results point to a scenario in which one heme may present two different coordination states, namely, His/Cys and His/Met, with this change in coordination being related to a possible catalytic activity of Cys46 in sulfur chemistry that is essential for DsrJ function.

Although the DsrMKJOP complex has been purified and characterized from *D. desulfuricans*, it is not clear whether DsrJ is an electron entry or exit point or a catalytic subunit (*5*). However, a more recent model of the function of the complex proposes electron transfer from the periplasm to the cytoplasm (*52*). Because the sulfur metabolisms of *D. vulgaris* and *A. vinosum* are the reverse of each other, one could assume that electron flow through the DsrMKJOP complex in *A. vinosum* proceeds from the cytoplasm to the periplasm. This could account for the difference in the heme redox potentials observed between DsrJ forms from the two organisms. To further examine the role of DsrJ in *A. vinosum*, complementation experiments with *dsrJ* from *D. vulgaris* were conducted. These experiments unambiguously show that the *dsrJ* gene from the sulfate reducer *D. vulgaris* can complement the *A. vinosum* Δ*dsrJ* mutant, restoring the wild-type phenotype. This experiment proved that despite the fact that *A. vinosum* DsrJ is only 34% similar to *D. vulgaris* DsrJ, the latter is able to substitute its homologue in *A. vinosum*, indicating that both can perform the same function in organisms with opposite sulfur metabolisms, i.e., sulfate reduction versus sulfur oxidation. Interesting in this respect is the pylogenetic distribution of the DsrMKJOP proteins. The proteins from the sulfur-oxidizing Chlorobiaceae are more closely related to the proteins from sulfate reducers than to *A. vinosum*, and horizontal gene transfer from the sulfate reducers to the Chlorobiaceae has been proposed (*3*).

The precise function of DsrJ remains unclear, and possible interaction partners in the periplasm are still unknown. On the basis of the unique nature of DsrJ with its unusual heme coordination, it is tempting to speculate that DsrJ has a catalytic function rather than only a function in electron transport. In such a scenario, DsrJ would participate in the oxidation of a putative sulfur substrate in the periplasm, probably involving Cys46, and the released electrons would be transported across the membrane via the other components of the DsrMKJOP transmembrane complex. In this context, it has to be noted that there are two DsrJ proteins in the database where cysteine 46 (*A. vinosum* numbering) is lacking and may be replaced with a histidine: the proteins from the endosymbionts of *Calyptogena magnifica* (Figure 1) and *Calyptogena okutanii*. Furthermore, the two methionines that are likely candidates for heme ligation of another heme are also missing (Figure 1). However, no experimental data concerning Dsr proteins are available for these organisms. Alternatively, the electrons could originate from a periplasmic interaction partner. Clearly, further studies on DsrJ will be necessary to clarify the structure and function of this unusual triheme cytochrome *c*.

ACKNOWLEDGMENT

Excellent technical assistance by Renate Zigann and Simone Waclawek is gratefully acknowledged. We also acknowledge Dr. Lígia Saraiva for kindly supplying the *D. vulgaris* chromosomal DNA and Dr. Ana Coelho for MS data at the Mass Spectrometry Laboratory. We thank the reviewers for their helpful comments and suggestions.

SUPPORTING INFORMATION AVAILABLE

Bacterial strains, plasmids, and primers used in this study (Table S1) and putative assignment of RR bands found in the $1000-1700\ cm^{-1}$ frequency region of DsrJ obtained with 647 nm excitation (Table S2). This material is available free of charge via the Internet at http://pubs.acs.org.

REFERENCES

1. Dahl, C., Engels, S., Pott-Sperling, A. S., Schulte, A., Sander, J., Lübbe, Y., Deuster, O., and Brune, D. C. (2005) Novel genes of the *dsr* gene cluster and evidence for close interaction of Dsr proteins during sulfur oxidation in the phototrophic sulfur bacterium *Allochromatium vinosum*. *J. Bacteriol. 187*, 1392–1404.
2. Schedel, M., Vanselow, M., and Trüper, H. G. (1979) Siroheme sulfite reductase isolated from *Chromatium vinosum*. Purification and investigation of some of its molecular and catalytic properties. *Arch. Microbiol. 121*, 29–36.
3. Sander, J., Engels-Schwarzlose, S., and Dahl, C. (2006) Importance of the DsrMKJOP complex for sulfur oxidation in *Allochromatium vinosum* and phylogenetic analysis of related complexes in other prokaryotes. *Arch. Microbiol. 186*, 357–366.
4. Haveman, S. A., Greene, E. A., Stilwell, C. P., Voordouw, J. K., and Voordouw, G. (2004) Physiological and gene expression analysis of inhibition of *Desulfovibrio vulgaris* Hildenborough by nitrite. *J. Bacteriol. 186*, 7944–7950.
5. Pires, R. H., Venceslau, S. S., Morais, F., Teixeira, M., Xavier, A. V., and Pereira, I. A. C. (2006) Characterization of the *Desulfovibrio desulfuricans* ATCC 27774 DsrMKJOP complex: A membrane-bound redox complex involved in the sulfate respiratory pathway. *Biochemistry 45*, 249–262.
6. Pereira, I. (2007) Respiratory membrane complexes of *Desulfovibrio*. In Microbial Sulfur Metabolism (Dahl, C., and Friedrich, C. G., Eds.) pp 24−35, Springer, Berlin.

7. Pott, A. S., and Dahl, C. (1998) Sirohaem sulfite reductase and other proteins encoded by genes at the *dsr* locus of *Chromatium vinosum* are involved in the oxidation of intracellular sulfur. *Microbiology 144*, 1881–1894.
8. Mander, G. J., Duin, E. C., Linder, D., Stetter, K. O., and Hedderich, R. (2002) Purification and characterization of a membrane-bound enzyme complex from the sulfate-reducing archaeon *Archaeoglobus fulgidus* related to heterodisulfide reductase from methanogenic archaea. *Eur. J. Biochem. 269*, 1895–1904.
9. Cheesman, M. R., Little, P. J., and Berks, B. C. (2001) Novel heme ligation in a *c*-type cytochrome involved in thiosulfate oxidation: EPR and MCD of SoxAX from *Rhodovulum sulfidophilum*. *Biochemistry 40*, 10562–10569.
10. Kappler, U., Aguey-Zinsou, K.-F., Hanson, G. R., Bernhardt, P. V., and McEwan, A. G. (2004) Cytochrome c_{551} from *Starkeya novella*: Characterization, spectroscopic properties, and phylogeny of a diheme protein of the SoxAX family. *J. Biol. Chem. 279*, 6252–6260.
11. Ogawa, T., Furusawa, T., Nomura, R., Seo, D., Hosoya-Matsuda, N., Sakurai, H., and Inoue, K. (2008) SoxAX binding protein, a novel component of the thiosulfate-oxidizing multienzyme system in the green sulfur bacterium *Chlorobium tepidum*. *J. Bacteriol. 190*, 6097–6110.
12. Rother, D., and Friedrich, C. G. (2002) The cytochrome complex SoxXA of *Paracoccus pantotrophus* is produced in *Escherichia coli* and functional in the reconstituted sulfur-oxidizing enzyme system. *Biochim. Biophys. Acta 1598*, 65–73.
13. Alric, J., Tsukatani, Y., Yoshida, M., Matsuura, K., Shimada, K., Hienerwadel, R., Schoepp-Cothenet, B., Nitschke, W., Nagashima, K. V. P., and Verméglio, A. (2004) Structural and functional characterization of the unusual triheme cytochrome bound to the reaction center of *Rhodovulum sulfidophilum*. *J. Biol. Chem. 279*, 26090–26097.
14. van Driessche, G., Devreese, B., Fitch, J. C., Meyer, T. E., Cusanovich, M. A., and Van Beeumen, J. J. (2006) GHP, a new *c*-type green heme protein from *Halochromatium salexigens* and other proteobacteria. *FEBS J. 273*, 2801–2811.
15. Maniatis, T., Fritsch, E. F., and Sambrook, J. (1982) Molecular cloning: A laboratory manual, Cold Spring Harbor Laboratory Press, Plainview, NY.
16. Blattner, F. R., Williams, B. G., Blechl, A. E., Denniston-Thompson, K., Faber, H. E., Furlong, L., Grunwald, D. J., Kiefer, D. O., Moore, D. D., Schumm, J. W., Sheldon, E. L., and Smithies, O. (1977) Charon phages: Safer derivatives of bacteriophage λ for DNA cloning. *Science 196*, 161–169.
17. Dahl, C. (1996) Insertional gene inactivation in a phototrophic sulphur bacterium: APS-reductase-deficient mutants of *Chromatium vinosum*. *Microbiology 142*, 3363–3372.
18. Ausubel, F. M., Brent, R., Kingston, R. E., Moore, D. D., Seidman, J. G., and Struhl, K. (1995) Current Protocols in Molecular Biology, Greene Publishing Associates and Wiley-Interscience, New York.
19. Horton, R. M. (1995) PCR-mediated recombination and mutagenesis. SOEing together tailor-made genes. *Mol. Biotechnol. 3*, 93–99.
20. Arslan, E., Schulz, H., Zufferey, R., Künzler, P., and Thöny-Meyer, L. (1998) Overproduction of the *Bradyrhizobium japonicum c*-type cytochrome subunits of the cbb_3 oxidase in *Escherichia coli*. *Biochem. Biophys. Res. Commun. 251*, 744–747.
21. Schägger, H. (2006) Tricine-SDS-PAGE. *Nat. Protoc. 1*, 16–22.
22. Thomas, P. E., Ryan, D., and Levin, W. (1976) An improved staining procedure for the detection of the peroxidase activity of cytochrome P-450 on sodium dodecyl sulfate polyacrylamide gels. *Anal. Biochem. 75*, 168–176.
23. Berry, E. A., and Trumpower, B. L. (1987) Simultaneous determination of hemes *a*, *b*, and *c* from pyridine hemochrome spectra. *Anal. Biochem. 161*, 1–15.
24. Todorovic, S., Jung, C., Hildebrandt, P., and Murgida, D. H. (2006) Conformational transitions and redox potential shifts of cytochrome P450 induced by immobilization. *J. Biol. Inorg. Chem. 11*, 119–127.
25. Lübbe, Y. J., Youn, H.-S., Timkovich, R., and Dahl, C. (2006) Siro(haem)amide in *Allochromatium vinosum* and relevance of DsrL and DsrN, a homolog of cobyrinic acid *a,c*-diamide synthase, for sulphur oxidation. *FEMS Microbiol. Lett. 261*, 194–202.
26. Pattaragulwanit, K., and Dahl, C. (1995) Development of a genetic system for a purple sulfur bacterium: Conjugative plasmid transfer in *Chromatium vinosum*. *Arch. Microbiol. 164*, 217–222.
27. Weaver, P. F., Wall, J. D., and Gest, H. (1975) Characterization of *Rhodopseudomonas capsulata*. *Arch. Microbiol. 105*, 207–216.
28. Dahl, C., Schulte, A., Stockdreher, Y., Hong, C., Grimm, F., Sander, J., Kim, R., Kim, S.-H., and Shin, D. H. (2008) Structural and molecular genetic insight into a widespread sulfur oxidation pathway. *J. Mol. Biol. 384*, 1287–1300.
29. Prange, A., Engelhardt, H., Trüper, H. G., and Dahl, C. (2004) The role of the sulfur globule proteins of *Allochromatium vinosum*: Mutagenesis of the sulfur globule protein genes and expression studies by real-time RT-PCR. *Arch. Microbiol. 182*, 165–174.
30. Rethmeier, J., Rabenstein, A., Langer, M., and Fischer, U. (1997) Detection of traces of oxidized and reduced sulfur compounds in small samples by combination of different high-performance liquid chromatography methods. *J. Chromatogr., A 760*, 295–302.
31. Kelly, D. P., Chambers, L. A., and Trudinger, P. A. (1969) Cyanolysis and spectrophotometric estimation of trithionate in mixture with thiosulfate and tetrathionate. *Anal. Chem. 41*, 898–901.
32. Yoshioka, S., Takahashi, S., Hori, H., Ishimori, K., and Morishima, I. (2001) Proximal cysteine residue is essential for the enzymatic activities of cytochrome P450cam. *Eur. J. Biochem. 268*, 252–259.
33. Martinis, S. A., Blanke, S. R., Hager, L. P., Sligar, S. G., Hoa, G. H., Rux, J. J., and Dawson, J. H. (1996) Probing the heme iron coordination structure of pressure-induced cytochrome P420cam. *Biochemistry 35*, 14530–14536.
34. Reijerse, E. J., Sommerhalter, M., Hellwig, P., Quentmeier, A., Rother, D., Laurich, C., Bothe, E., Lubitz, W., and Friedrich, C. G. (2007) The unusal redox centers of SoxXA, a novel *c*-type heme-enzyme essential for chemotrophic sulfur-oxidation of *Paracoccus pantotrophus*. *Biochemistry 46*, 7804–7810.
35. Cheesman, M. R., Ferguson, S. J., Moir, J. W., Richardson, D. J., Zumft, W. G., and Thomson, A. J. (1997) Two enzymes with a common function but different heme ligands in the forms as isolated. Optical and magnetic properties of the heme groups in the oxidized forms of nitrite reductase, cytochrome cd_1, from *Pseudomonas stutzeri* and *Thiosphaera pantotropha*. *Biochemistry 36*, 16267–16276.
36. van Wonderen, J. H., Knight, C., Oganesyan, V. S., George, S. J., Zumft, W. G., and Cheesman, M. R. (2007) Activation of the cytochrome cd_1 nitrite reductase from *Paracoccus pantotrophus*. Reaction of oxidized enzyme with substrate drives a ligand switch at heme *c*. *J. Biol. Chem. 282*, 28207–28215.
37. Allen, J. W., Watmough, N. J., and Ferguson, S. J. (2000) A switch in heme axial ligation prepares *Paracoccus pantotrophus* cytochrome cd_1 for catalysis. *Nat. Struct. Biol. 7*, 885–888.
38. Siebert, F., and Hildebrandt, P. (2008) Vibrational spectroscopy in life science, Wiley-VCH Verlag GmbH & Co KGaA, Weinheim, Germany.
39. Todorovic, S., Verissimo, A., Wisitruangsakul, N., Zebger, I., Hildebrandt, P., Pereira, M. M., Teixeira, M., and Murgida, D. H. (2008) SERR-spectroelectrochemical study of a cbb3 oxygen reductase in a biomimetic construct. *J. Phys. Chem. B 112*, 16952–16959.
40. Pereira, I. A. C., and Xavier, A. V. (2005) Multi-heme *c* cytochromes and enzymes. In Encyclopedia of Inorganic Chemistry (King, R. B., Ed.) pp 3360−3376, Wiley, New York.
41. Aubert, C., Guerlesquin, F., Bianco, P., Leroy, G., Tron, P., Stetter, K.-O., and Bruschi, M. (2001) Cytochromes c_{555} from the hyperthermophilic bacterium *Aquifex aeolicus*. 2. Heterologous production of soluble cytochrome $c_{555}{}^{s}$ and investigation of the role of methionine residues. *Biochemistry 40*, 13690–13698.
42. Barker, P. D., Nerou, E. P., Cheesman, M. R., Thomson, A. J., de Oliveira, P., and Hill, H. A. O. (1996) Bis-methionine ligation to heme iron in mutants of cytochrome b_{562}. 1. Spectroscopic and electrochemical characterization of the electronic properties. *Biochemistry 35*, 13618–13626.
43. Paoli, M., Marles-Wright, J., and Smith, A. (2002) Structure-function relationships in heme-proteins. *DNA Cell Biol. 21*, 271–280.
44. Reedy, C. J., Elvekrog, M. M., and Gibney, B. R. (2008) Development of a heme protein structure electrochemical function database. *Nucleic Acids Res. 36,* database issue D307–D313.
45. Nakajima, H., Honma, Y., Tawara, T., Kato, T., Park, S.-Y., Miyatake, H., Shiro, Y., and Aono, S. (2001) Redox properties and coordination structure of the heme in the CO-sensing transcriptional activator CooA. *J. Biol. Chem. 276*, 7055–7061.
46. Ran, Y., Zhu, H., Liu, M., Fabian, M., Olson, J. S., Aranda, R., Phillips, G. N., Dooley, D. M., and Lei, B. (2007) Bis-methionine ligation to heme iron in the streptococcal cell surface protein Shp facilitates rapid hemin transfer to HtsA of the HtsABC transporter. *J. Biol. Chem. 282*, 31380–31388.
47. Kappler, U., Bernhardt, P. V., Kilmartin, J., Riley, M. J., Teschner, J., McKenzie, K. J., and Hanson, G. R. (2008) SoxAX cytochromes, a new type of heme copper protein involved in bacterial energy generation from sulfur compounds. *J. Biol. Chem. 283*, 22206–22214.
48. Friedrich, C. G., Bardischewsky, F., Rother, D., Quentmeier, A., and Fischer, J. (2005) Prokaryotic sulfur oxidation. *Curr. Opin. Microbiol. 8*, 253–259.
49. Kelly, D. P., Shergill, J. K., Lu, W. P., and Wood, A. P. (1997) Oxidative metabolism of inorganic sulfur compounds by bacteria. *Antonie van Leeuwenhoek 71*, 95–107.

50. Bamford, V. A., Bruno, S., Rasmussen, T., Appia-Ayme, C., Cheesman, M. R., Berks, B. C., and Hemmings, A. M. (2002) Structural basis for the oxidation of thiosulfate by a sulfur cycle enzyme. *EMBO J. 21*, 5599–5610.
51. Dambe, T., Quentmeier, A., Rother, D., Friedrich, C., and Scheidig, A. J. (2005) Structure of the cytochrome complex SoxXA of *Paracoccus pantotrophus*, a heme enzyme initiating chemotrophic sulfur oxidation. *J. Struct. Biol. 152*, 229–234.
52. Oliveira, T. F., Vonrhein, C., Matias, P. M., Venceslau, S. S., Pereira, I. A. C., and Archer, M. (2008) The crystal structure of *Desulfovibrio vulgaris* dissimilatory sulfite reductase bound to DsrC provides novel insights into the mechanism of sulfate respiration. *J. Biol. Chem. 283*, 34141–34149.